



In situ monitoring of used-sand regeneration in foundries by impedance spectroscopy

Luca Bifano¹, Marco Weider², Alice Fischerauer¹, Gotthard Wolf², and Gerhard Fischerauer¹

¹Chair of Measurement and Control Systems, University of Bayreuth, 95447 Bayreuth, Germany

²Foundry Institute of the TU Freiberg, TU Bergakademie Freiberg, 09599 Freiberg, Germany

Correspondence: Luca Bifano (luca.bifano@uni-bayreuth.de)

Received: 26 October 2021 – Revised: 26 August 2022 – Accepted: 26 September 2022 – Published: 11 October 2022

Abstract. This work deals with the impedimetric monitoring of used-sand regeneration in the foundry industry. During the regeneration of used sand, a quartz sand similar to new sand is produced from already used molding and core sand, which especially serves to produce new cores. We explore whether the regeneration progress can be assessed in situ based on measured impedance spectra and their features. The impedances of plate capacitors filled with different typical used-sand mixtures, consisting of quartz sand, coal dust, and bentonite, were repeatedly measured in a frequency range from 500 Hz to 1 MHz. The reproducibility of the measurements proved to be sufficient for practical applications. The mean impedances were plotted in Nyquist diagrams. From these plots, systematic impedance–composition correlations could be determined for two of the three component systems. Conclusions about the regeneration state could be drawn from the impedance curves by introducing various features. These were the median, the mean, and the standard deviation of the frequency-dependent resistance and reactance. With these indicators, it was then possible to establish one-to-one relations between the material composition of the molding materials and the impedance measurement. In field measurements on regenerated used sands, this observation was confirmed, and the regeneration progress was observed on the basis of the impedimetrically determined characteristic data.

1 Introduction

The foundry industry is an energy- and resource-intensive branch of industry. This calls for solutions that make the various process stages more environmentally compatible. If one looks at the published environmental reports of foundries, it becomes apparent that, in addition to the metal used, it is primarily water and the raw materials for mold and core production that are consumed in the production of castings (Denes, 2019). These raw materials include quartz sand as the basic molding material, bentonite as an inorganic molding material binder, and other additives (Tilch et al., 2019). Quartz sand is increasingly difficult to supply due to the quality requirements of the various applications, as the sand must be of the quality desired for the various industrial processes, such as the construction sector or the foundry industry. Also, the worldwide annual sand production of about 40×10^9 t of sand and gravel exceeds the natural regeneration of the resource by a factor of 2, so that a secure supply of raw ma-

terials will become more difficult in the future (Götze and Göbbels, 2017; Peduzzi, 2014). Not only the supply of raw materials, but also waste disposal is developing critically in the foundry industry. When new sand is used, a corresponding amount of already used sand must be disposed of at the same time, usually by landfilling it (Tilch et al., 2019). In Germany, however, the number of landfills is continuously decreasing, while the amount of waste is increasing, which will make it more difficult to dispose of used sand in the future (Statista, 2020, 2022). This established raw material use corresponds to the linear type (Fig. 1).

In order to alleviate the procurement and disposal problems, it makes sense to no longer arrange raw material use in a linear but instead in a circular structure (Fig. 2).

The resulting raw material or sand cycle is closed, which offers not only environmental but also economic advantages. In the area of molding material, for example, the procurement of the input materials and the disposal are responsi-

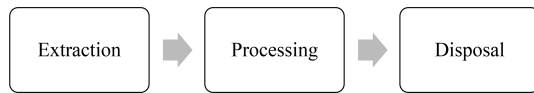


Figure 1. Linear raw material usage from left to right.

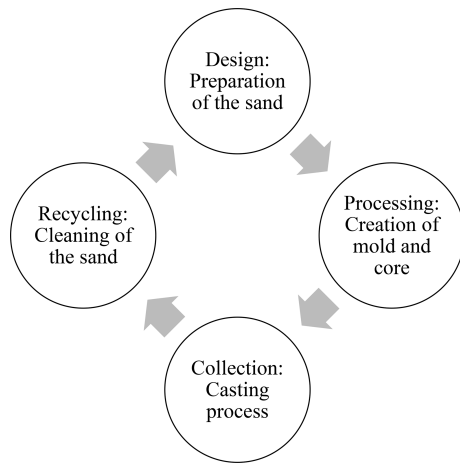


Figure 2. Circular raw material utilization (raw material cycle) with the sand cycle from the foundry industry as an example.

ble for approximately 50% of the total cost (Tilch et al., 2019). This favors the use of regeneration processes and plants as part of the recycling step of Fig. 2, which produce a new sand-like substitute product from used sand (Denes, 2019). Data from Germany show the dimension of the economic and environmental potential of a functioning used-sand regeneration: in 2020, there were 506 foundries in Germany (China: 26 000), of which 140 were iron foundries (China: 14 000) (Statista, 2020a, b). One of these plants required 46 349 t of virgin sand, 5028 t of inorganic binder, and 5949 t of additives for its mold and core production this year. In the same year, a total of 47 160 t of molding waste had to be disposed of (Denes, 2019).

In order to be able to operate these regeneration plants optimally, adequate possibilities of process control with corresponding concepts of process monitoring must be developed. The aim is to replace the corresponding laboratory tests of the molding material, which are described in Tilch et al. (2019) and various foundry standards, with suitable in situ process solutions so that online monitoring of the molding material condition and direct intervention in the process control are possible.

Among the first non-standardized measurement methods for monitoring sand properties are, for example, methods based on microwave technology (Opyd and Granat, 2015; Stachowicz, 2016). The actual aim of these investigations is to determine the power component of the microwave that leads to the heating of the sand-binder mixture. The main area of investigation is sand-binder mixtures whose curing process is thermally activated. As a by-product of this re-

search, it has been shown that, in particular, the reflected microwave power contains information about the density of the molding material bulk (Stachowicz, 2016). Other groups in the field of microwave technology use the disturbance of cavity resonators to investigate material properties of molding sands (Opyd and Granat, 2015). Other approaches deal with the introduction of traditional sensor technology, such as thermocouples, in order to be able to follow thermal processes during casting. The measured data obtained in this way can then be evaluated using inverse Fourier thermal analysis. However, this method is still limited to initial trials in test molds and cores (Toth et al., 2016). In contrast to the classical laboratory analysis methods, microwave methods are suitable for process monitoring due to their low measurement time. However, a metallic cavity is needed in which a standing electromagnetic wave can form. Metal tools moving inside a process complicate this requirement. In addition, this measurement method is limited to dielectric materials, whose relative permittivity must not be too high and, if possible, must not exhibit any electrical conductivity (Balmus et al., 2006). Also, one has to keep an eye on the information density because one typically measures the resonant frequency of the cavity and infers the relative permittivity of the material from it; i.e., one obtains only one data point (Opyd and Granat, 2015).

In this respect, electrical impedance spectroscopy (EIS) offers some advantages. Depending on the number of frequency points used, a high information density is obtained with a sufficiently short measurement time. It is also no longer necessary to restrict the method to a class of materials with certain material properties, which leads to a greater number of possible applications. Since EIS is also noninvasive and nondestructive and provides a spatially integral measurement result, we believe it is suitable for process monitoring of used-sand regeneration. For this reason, we explore the capabilities of impedance spectroscopy as a basis of a system for the process monitoring of used-sand regeneration and as an indicator of the regeneration progress (Bifano et al., 2020).

The molding material occurring in the regeneration process consists of quartz sand, bentonite as an inorganic binder, and additives such as coal dust (Tilch et al., 2019). The conductive and dielectric properties of these materials have already been investigated by a number of research groups, although not with a focus on the possibility of technical application but in basic areas of chemistry and geology. For example, bentonite is interesting for environmental applications in landfill construction or in the pharmaceutical and agricultural fields due to its large specific active surface area, high absorption capacity, high binding capacity, and good swelling ability (Götze and Göbbels, 2017; Kaden et al., 2013). The scientific investigation of the influence of material properties, such as chain length, cation structure, and density in bentonite, on the binding behavior of water molecules at the bentonite surface also reflects these fields of applica-

tion. For this purpose, the frequency, polarization, and relaxation behaviors of the dielectric permittivity of bentonite were considered. It was found that the complex dielectric permittivity was systematically affected by different concentrations of metal ions in the structure of bentonite (Chu et al., 2019). Other studies showed that correlations exist between the porosity of a bulk material and the relative dielectric permittivity (Robinson and Friedman, 2003) or the electrical conductivity (Chu et al., 2019). In Belyaeva et al. (2017) and Al Rashid et al. (2018), theories were published that allow conclusions to be drawn about the different bonding states of water molecules to sand–bentonite–water mixtures through measured impedances of samples. These results suggest that impedance spectroscopy is fundamentally suitable for analyzing bulk or grainy materials and using the obtained data for process monitoring. Advantages of impedance spectroscopy compared to other measurement methods are the integral measurement result, which suppresses the influence of outliers to a large extent, and the noninvasive, fast, and flexible measurement. The latter properties are due to the fact that the frequency range can be adjusted to the respective requirements.

In previous work, our aim was to evaluate whether the state-of-the-art impedimetric results can be transferred to the application case of the foundry industry. This showed that measurable impedance spectra were systematically related to the molding material composition (Bifano et al., 2020). The measurement data were also reproducible (Bifano et al., 2021). Both of these results underline the potential of impedance spectroscopy for use as an in situ process measurement technique in the sand cycle of the foundry industry. In this work, we demonstrate the suitability of various features or indicators extracted from impedance spectra for the task of observing the sand condition during used-sand regeneration. Typical used-sand compositions were prepared and their impedances measured under laboratory conditions. The suitability of the features selected was then verified by field measurements on a regenerator.

2 State of the art

Figure 2 shows the simplified molding material cycle. In the first process step, the molding material is prepared; i.e., quartz sand, binder, water, and additives are mixed together. In the second stage, a two-part mold is created using a positive pattern of the later casting. At the same time, the core is made, placed in the resulting lower half of the mold, and the structure is closed by the upper half of the mold. In the next step, the cast product is created by pouring the liquid metal into the created mold structure. After the metal has cooled and hardened, the casting is unpacked from the mold, and the used molding material is collected. This is then made to a large extent usable again in various cleaning steps and returns to the preparation stage as so-called recirculating material

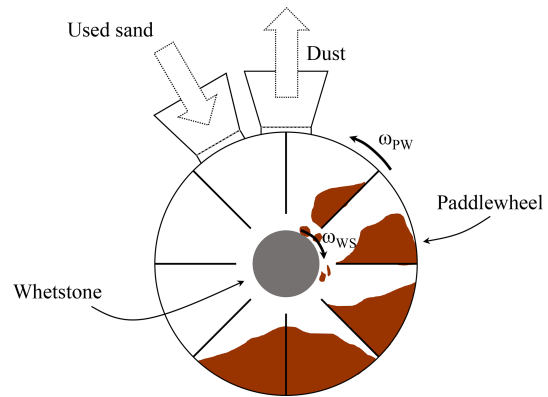


Figure 3. Mechanical regenerator according to Wijnker (2014). Such a regenerator was also used in our field tests.

(step 1). However, the core production, in particular, requires new sand and also uses other binder types than those used in the mold. The continuous use of new sand in the core sand area would result in increasingly large quantities of recirculating sand circulating in a foundry as time goes on. For this reason, either a portion of the circulating sand corresponding to the new sand used in the core area must be removed from the system and disposed of as waste, or it must be processed in such a way that it can be used as a new sand substitute in the core sand area. This processing is called regeneration and takes place in mechanical regenerators (Fig. 3) and/or thermal regenerators. This work focuses on mechanical regenerators.

The aim of a mechanical regeneration system is to remove the inactive binder shells burned onto the sand grain surface so that ideally the pure sand grain remains as the regeneration product at the end. In addition, all active binder components must also be removed from the molding material during regeneration. All dust components are removed from the system via the exhaust system. Depending on the manufacturer, the system design varies. In the center of the regenerator in Fig. 3 there is a whetstone which removes the binder shells from the sand particles. A paddle wheel runs around it in the same or opposite direction, which conveys the used sand to the whetstone. The resulting dust is extracted from the plant by means of suction. This type of plant can only be operated in batch mode; i.e., the used sand is filled into the plant, the process is run for a certain time, and at the end the product, the reclaim, is removed. To date, the time required for full regeneration cannot be predicted reliably as it depends on unknown process details and as the process cannot be adjusted accordingly. The state-of-the-art process consists of three stages: (1) pre-dedusting – only the paddle wheel rotates, and loose dust particles are removed from the used sand and extracted via the suction system; (2) grinding – now the whetstone also rotates (either with the bucket wheel or contrariwise), and dust particles generated by the grinding action are removed from the processed molding material

by suction; (3) post-dedusting – the whetstone stops, and, as in (1), only the paddle wheel rotates. Dust particles generated by the grinding and not yet extracted are now removed from the reclaim.

The regeneration is assessed by characteristic values, such as the degree of regeneration, the yield of regeneration or the degree of reuse. The reclaim quality can be determined on the basis of the new sand requirements from the relevant standards (Wijnker, 2014). Laboratory measurements can be used to determine granulometric parameters or physical-technological properties, such as loss on ignition, active clay content or slurry content, which can then be used to draw conclusions about the regeneration condition (Tilch et al., 2019; Wijnker, 2014). Direct process monitoring is not available to date. In other branches of industry, such as additive manufacturing, the first in-line measurement methods have been established which, similar to impedance spectroscopy, use the complex dielectric permittivity as a measured variable (Fieber et al., 2020). This can be a model for the current application.

It is well known that EIS can be used to characterize various material properties. For example, Van de Leur and Zevenhoven (1991) show that the apparent impedance of corundum and mullite bulk material samples reveals up to three material-specific relaxation processes in the frequency range from 0.1 Hz to 10 kHz. Since these materials are similar to classical molding materials, this suggests that EIS is also suitable for monitoring used-sand regeneration. However, the previous results were all obtained under laboratory conditions. When EIS is transferred to the field, new challenges arise owing to a large number of disturbances due to, e.g., geometry variations, temperature fluctuations, and mechanically harsh environmental conditions. This raises the question as to whether it is possible to generate the impedimetric data reliably enough to allow for significant conclusions about the material composition.

3 Measuring system and regeneration settings

The measurement setup used consisted of a desktop PC, an Agilent E4980A LCR meter, and two measuring cells (Fig. 4).

The LCR meter can be addressed via a USB connection through the PC. This task is performed by an application-specific LabView program, via which all measurement settings can be made, and the measurement can be controlled. The measuring cell is connected to the LCR meter via two coaxial cables. Figure 5 shows the two measuring cells used.

On the one hand, a plate capacitor (diameter of the electrodes – 13 cm, electrode spacing – 4 cm) was used as the measuring cell (Fig. 5a). On the other hand, a cylindrical capacitor was used (Fig. 5b). As it was found that the latter could cover a greater variety of regenerator types (geometries exist other than the one shown in Fig. 3), it was decided

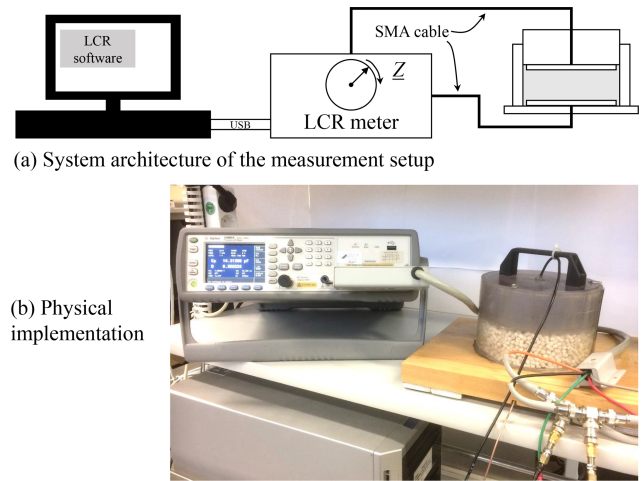


Figure 4. Measurement setup consisting of a PC, the LCR meter, and the measuring cell: (a) system architecture and (b) physical implementation (Bifano et al., 2021).

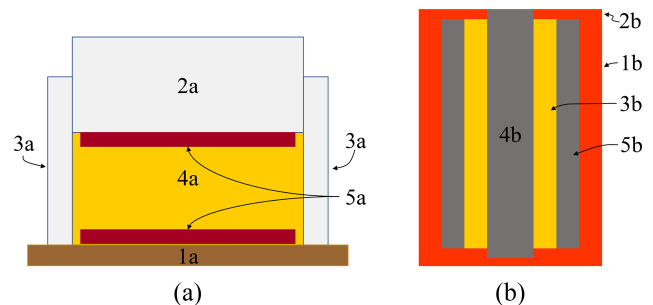


Figure 5. Measuring cells of the plate-capacitor type (a) (Bifano et al., 2020, 2021) and the cylindrical-capacitor type (b) (Hilzenthaller et al., 2021). The structure is as follows: wooden base plate (1a), Makrolon[®] stamp (2a), polymer casing (3a), molding material (4a), circular plate electrodes made of copper (5a), polymer casing (1b), polymer cover (2b), molding material (3b), inner electrode (4b), and outer electrode (5b) made of aluminum.

to carry out field measurements with the cylindrical capacitor (electrode height – 10 cm, electrode spacing – 1 cm). One advantage of using different types of measuring cells is that the dependence of the extracted features for regeneration monitoring on the measuring cell geometry can be estimated.

The laboratory tests necessary for the extraction of impedance characteristics were carried out with the aid of “artificially” prepared used-sand mixtures and the plate capacitor. Table 1 lists the different mixtures. This list does not cover the entirety of possible used-sand compositions (depending, among other things, on the foundry and casting product) but is meant to reflect typical substances and their compositions in used sand.

MUT 1a and 1b represent the target values, since both materials are pure quartz sand, and both MUTs can be used equally in the foundry, with MUT 1b obtained by heating

Table 1. Composition of the used-sand mixtures (material under test, MUT). MUT 1a and 1b serve as target values. These mixtures were measured with the measuring cell from Fig. 5a.

MUT	Material composition in percent					
	Quartz sand			Bentonite		Color of the representations in Figs. 6 to 9
	New	Used	Carbon dust	Active	Inactive/ dead	
1a	100					Green
1b		100				Orange
2a	99		1			Blue
2b	95		5			Red
2c	90		10			Black
3a	99			1		Blue
3b	95			5		Red
3c	90			10		Black
4a	45	45	5		5	Turquoise
4b	42.5	42.5	10		5	Red
4c	42.5	42.5	5		10	Blue
4d	40	40	10		10	Black

MUT 1a to 800 °C. This temperature is supposed to correspond to the average temperature that quartz sand experiences during casting (Tilch et al., 2019). The same procedure was followed for the inactivation of the bentonite of MUT 4a to 4d. Because the proportion of molding sand that is thermally loaded to such an extent that carbon and bentonite are destroyed is small, no mixture that has been completely heated to 800 °C has been investigated in the laboratory tests (Table 1). Such a used-sand mixture, which was completely thermally destroyed, does not exist in the industrial application. Therefore, an investigation of such mixtures was not carried out. Each MUT was filled into the measuring cell of Fig. 5a, and the frequency sweep from 500 Hz to 1 MHz, consisting of 145 frequency points, was run through 20 times and emptied again. This procedure was repeated 10 times, so that 10 × 20 data series with 145 data points each were collected for all MUTs. The frequency range was chosen based on the consideration that the required duration of a frequency sweep should be kept below 1 min to be compatible with the process dynamics (frequencies as low as a few hertz (Hz) or millihertz (mHz) are not useful here, unlike in battery technology). The following settings were made for the field measurement on the regenerator: a typical used sand from a foundry was used as the starting product. The batch size was 150 kg. Two batches of the same used sand were regenerated, with the rotational speed of the whetstone being 1830 rpm for batch 1 and 3190 rpm for batch 2. Conversely, this meant that batch 1 was regenerated with less energy than batch 2. The regeneration of each batch went through the regeneration pattern described above with pre-dedusting, grinding, and post-dedusting. After a defined time interval within the regeneration, a sample was drawn from the regenerator and characterized impedimetrically. Table 2 shows the respective measurement times (MTPs).

Table 2. Measurement times at which a regenerate sample was drawn from the regenerator and characterized impedimetrically. The samples belonging to these MTPs were measured with the measuring cell from Fig. 5b.

Measurement time points (MTPs)	Operation	Symbol colors in Figs. 10 to 12
MTP 0	Used sand	Red
MTP 1	5 min pre-dedusting	Black
MTP 2	10 min grinding	Blue
MTP 3	20 min grinding	Turquoise
MTP 4	30 min grinding	Pink
MTP 5	10 min post-dedusting	Green

MTP 5 corresponds to the finished reclaim, which is to be reused as a new sand replacement. The frequency vector used for the impedimetric measurements remained the same. Only the number of repetitions was reduced, resulting in 5 × 5 data series for each batch and each MTP during the field test. The entire presentation and evaluation of the measurement data was carried out in MATLAB. The vibrations occurring in the regeneration process probably influence the measurement result. In the analysis presented here, however, it should first be investigated whether the procedure described in this article is suitable for observing the regeneration progress. The disturbance of the measurement by vibrations has not yet been investigated and must be part of further investigations.

All measurements took place at a laboratory temperature of approx. 25 °C. Further investigations at temperatures up to 55 °C showed that a systematic temperature effect on the features extracted later from the impedance data in this paper could not be observed. Thus, these features seem to be temperature stable for the investigated samples. A maximum temperature of 55 °C was chosen because the regenerator manufacturer specifies an upper limit for the temperature of 60 °C and an optimum working window for regeneration of 20 to 40 °C.

4 Measurement data

Based on the investigations in Bifano et al. (2020), it is clear that the impedance spectra of different molding sand mixtures are systematically related to the molding sand composition. However, it is not yet known whether these correlations can be resolved finely enough to characterize typical used-sand compositions with these data. Verification of the method in the field is also lacking.

It was demonstrated in Bifano et al. (2021) that the impedance spectra of different measurement-cell fillings scatter in such a way that the respective mean values suffice for a first consideration of the molding compounds listed in Table 1. Figure 6 shows such average spectra for the various MUTs investigated. For completeness, the relative uncertain-

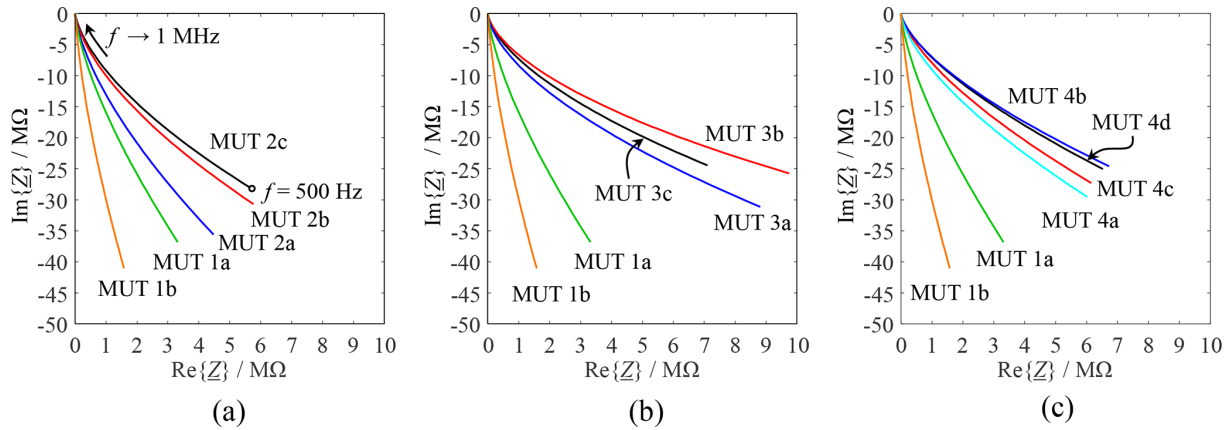


Figure 6. Nyquist curves of measurement-cell impedances with new and old quartz sand (a–c), quartz sand–carbon mixtures (a), quartz sand–bentonite mixtures (b), and quartz sand–carbon–bentonite mixtures (c) in the frequency range from 500 Hz to 1 MHz.

Table 3. Relative uncertainties in the real and imaginary parts of the MUT impedances and the associated frequencies, at a confidence level of 95 %.

MUT	Relative uncertainty and associated frequencies			
	Real part (%)	Frequency (kHz)	Imaginary part (%)	Frequency (kHz)
1a	3.19	1.20	0.57	0.50
1b	9.13	0.52	0.73	0.50
2a	5.09	1.80	1.58	0.50
2b	8.95	1.20	2.77	0.50
2c	5.63	1.40	2.40	0.50
3a	4.63	0.88	1.15	0.50
3b	5.45	4.20	2.97	0.50
3c	13.40	3.40	5.38	0.50
4a	12.09	2.20	4.05	0.50
4b	8.47	2.40	3.96	0.50
4c	9.48	2.00	4.10	0.50
4d	9.10	4.00	4.08	0.50

Table 4. Equations of the mean and standard deviation features for the real and imaginary parts of the impedance spectrum. The index i is the running variable of the 201 points of the impedance spectrum (Toutenburg and Heumann, 2008).

	R/Ω	X/Ω
Mean	$\frac{1}{201} \sum_{i=1}^{201} R_i$	$\frac{1}{201} \sum_{i=1}^{201} X_i$
Standard deviation	$\sqrt{\frac{1}{200} \sum_{i=1}^{201} (R_i - \bar{R})^2}$	$\sqrt{\frac{1}{200} \sum_{i=1}^{201} (X_i - \bar{X})^2}$

ties in the real and imaginary parts of the MUT impedances that emerged in the 10×20 measurement series over the entire frequency range are given in Table 3 according to Paradowski (1997). The frequency at which this maximum value occurs is also listed.

The results support the investigations from Bifano et al. (2021) in that the measurement is not overly sensitive to repeated emptying and refilling of the measuring cell. It must be considered that the mixture of a MUT filled into the measuring cell varies with repeated filling. A possible rationale is given in Bifano et al. (2021). Figure 6 clearly shows that although slight differences can be seen in the Nyquist diagram depending on the composition of the MUT, a systematic change in the Nyquist curves does not occur for all MUTs.

For this reason, we decided to extract features from the impedance spectra that form a systematic relationship with the regeneration progress. More specifically, the median, mean, and standard deviation of the impedance spectrum obtained by one frequency sweep were used as features. The median value is defined as the value that divides the spectrum into two halves. In this case with 201 spectrum points, 100 points are below and 100 points above the median value (Toutenburg and Heumann, 2008). This median determination applies to both the spectrum of the real and imaginary part. The calculation of the other features can be taken from Table 4.

Every feature is then represented by a single data point in the complex impedance plane. The 200 repeated measurements with a given MUT provided three sets of 200 such feature points (Figs. 7 to 9). The ellipses in the plots represent the empirical standard deviation of the feature points and are meant to guide the reader’s eye. Essentially, the ellipses belonging to different molding material mixtures overlap hardly or not at all. This serves as basis for an automatic classification of material compositions and material conditions, for example, by machine learning methods. We remind the reader that MUT 1a and b in Figs. 7 to 9 represent the regeneration target. The plots indicate that, with progress-

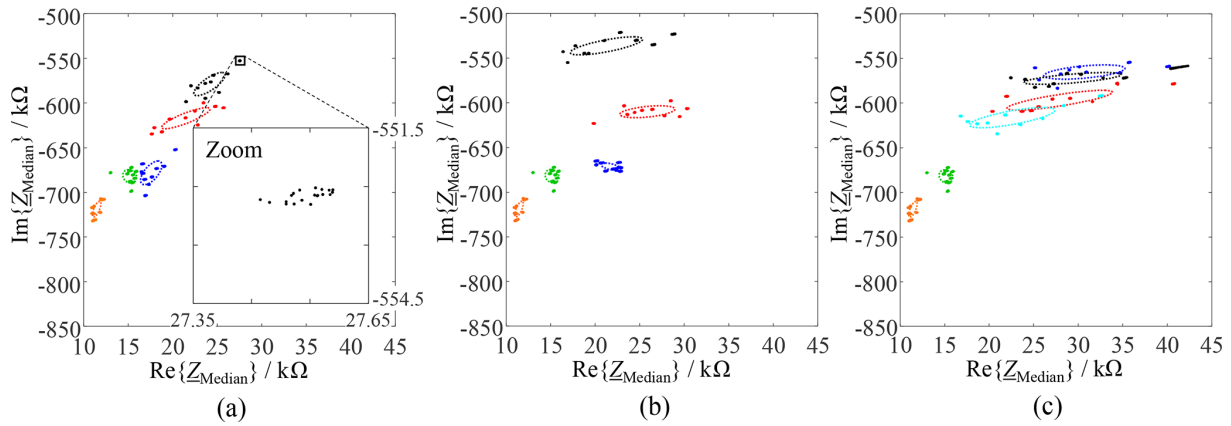


Figure 7. Distribution of the “median” feature for repeated measurements of various MUTs. Color coding as in Fig. 6. (a) MUT 1a and b and MUT 2a to c. (b) MUT 1a and b and MUT 3a to c. (c) MUT 1a and b and MUT 4a to d. The 20 repeated measurements with a given cell filling scatter so little that the 20 individual points can hardly be resolved in this representation. The zoomed-in view in (a) provides a better resolution of one point cloud by way of an example.

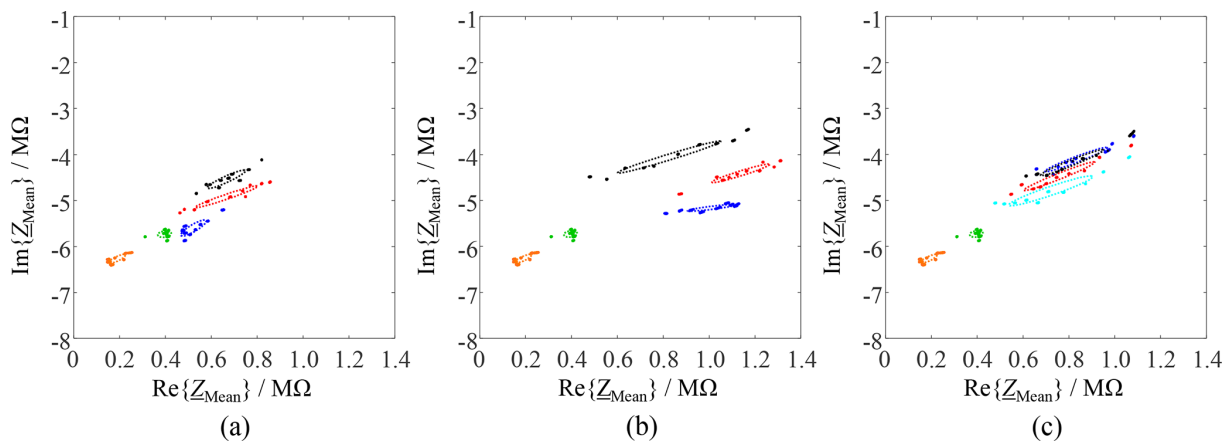


Figure 8. Distribution of the “mean” feature for repeated measurements of various MUTs. Color coding as in Fig. 6. (a) MUT 1a and b and MUT 2a to c. (b) MUT 1a and b and MUT 3a to c. (c) MUT 1a and b and MUT 4a to d.

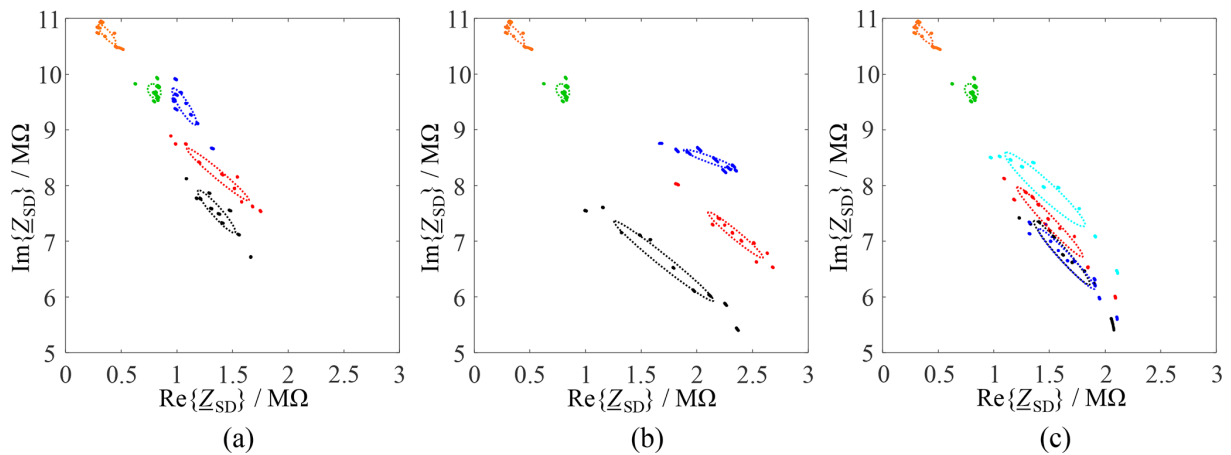


Figure 9. Distribution of the “standard deviation” feature for repeated measurements of various MUTs. Color coding as in Fig. 6. (a) MUT 1a and b and MUT 2a to c. (b) MUT 1a and b and MUT 3a to c. (c) MUT 1a and b and MUT 4a to d.

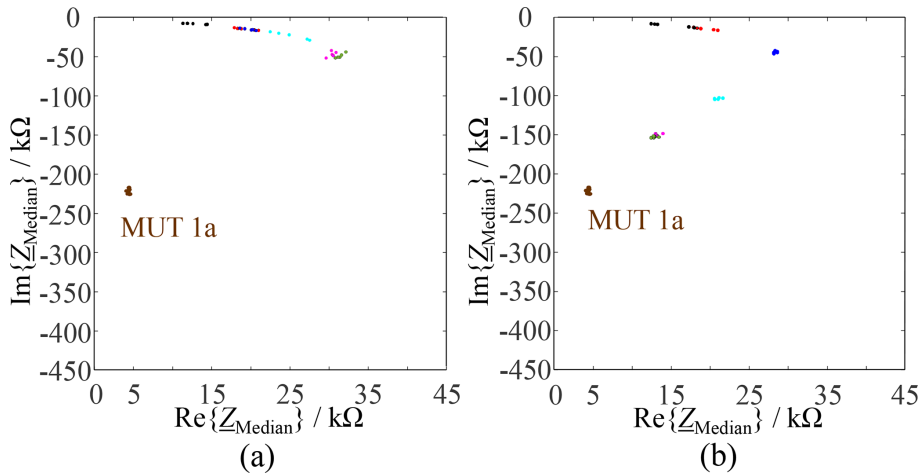


Figure 10. “Median” feature measured in the field. (a) Batch 1. (b) Batch 2.

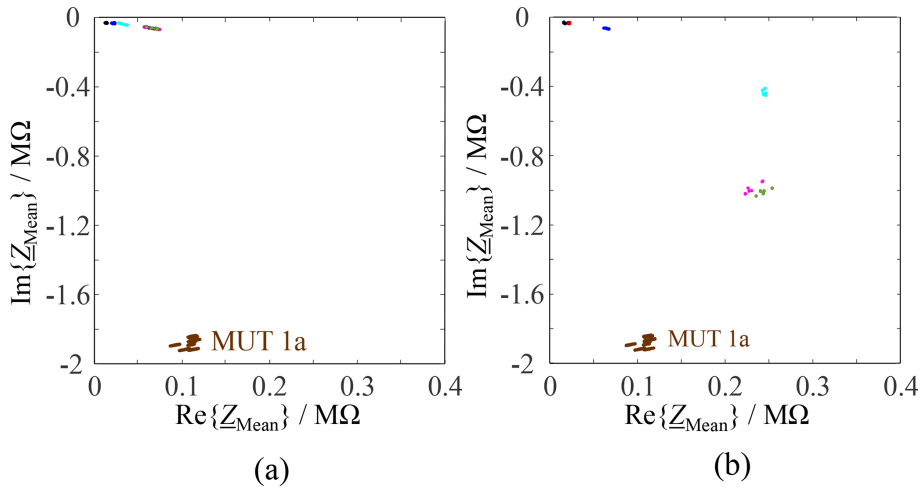


Figure 11. “Mean” feature measured in the field. (a) Batch 1. (b) Batch 2.

ing regeneration, the feature points “gravitate” to the target points. This is explained by the fact that the regeneration removes constituents, such as coal dust or bentonite, from the molding material. As a result, the material approaches the state of pure quartz sand more and more.

The MUTs listed in Table 1 are artificially produced used-sand mixtures which do not perfectly correspond to used sand from the field. This is particularly due to the mix quality, which does not resemble that in the field, and to the bentonite state, which, despite the temperature load, is not sintered onto the sand grain as in the casting process due to the lack of pressure from the molding plant and the liquid metal. Therefore, in order to check the field suitability of our approach, field measurements were carried out on molding material samples of a regeneration according to the time pattern from Table 2 on two batches which were respectively regenerated at low and high whetstone speeds (batch 1 and 2). The

key figures extracted from these data are shown in Figs. 10 to 12.

The scatter of these measurement results was again investigated as described above. The relative uncertainties in the real and imaginary parts of the impedances are listed in Table 5.

The numbers given in Table 5 demonstrate that the field data show a similar pattern of scatter as the laboratory data. This furnishes evidence for the reproducibility of the method. Since the presented features will be used to monitor regeneration, the relative uncertainties obtained from the feature data are listed in Table 6 for completeness.

The uncertainty values in Table 6 also show low values, which was to be expected since the impedance data from which the features were obtained already seemed reproducible. Thus, monitoring the regeneration process seems possible with the help of the presented features.

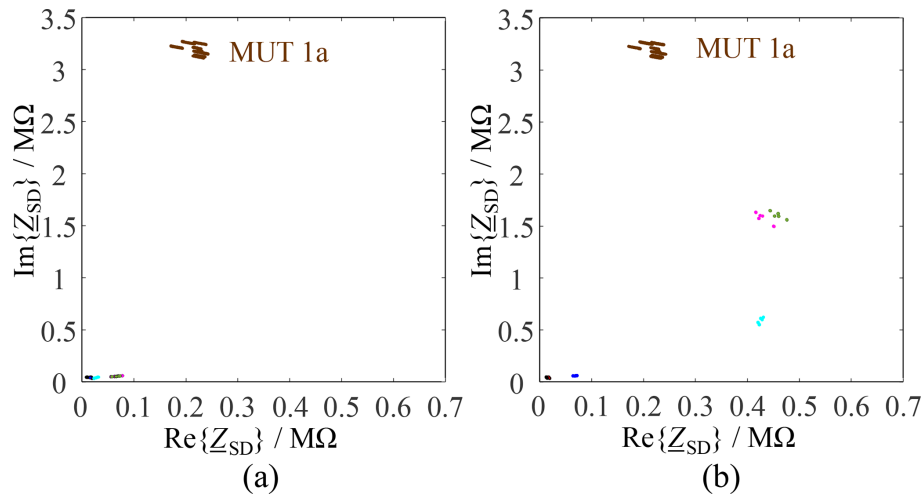


Figure 12. “Standard deviation” feature measured in the field. (a) Batch 1. (b) Batch 2.

Table 5. Relative uncertainties in the real and imaginary parts of the field-measured MUT impedances at various regeneration states and the associated frequencies, at a confidence level of 95 %.

MUT	Relative uncertainty and associated frequencies			
	Real part (%)	Frequency (kHz)	Imaginary part (%)	Frequency (kHz)
MTP 0	7.30	0.50	7.36	0.50
MTP 1, batch 1	10.53	0.50	8.96	66.00
MTP 2, batch 1	4.73	3.00	5.46	22.00
MTP 3, batch 1	11.83	5.40	14.48	18.00
MTP 4, batch 1	8.23	1.40	9.51	5.80
MTP 5, batch 1	6.48	1.60	7.66	6.60
MTP 1, batch 2	13.64	14.00	16.17	48.00
MTP 2, batch 2	2.80	1.80	3.13	7.20
MTP 3, batch 2	1.45	10.00	3.79	0.50
MTP 4, batch 2	2.77	5.80	2.35	0.50
MTP 5, batch 2	2.42	5.40	1.50	0.50

5 Analysis and discussion

Both in the measurement of the MUT (Table 3) and in the examination of the field samples (Table 5), the precision of the measured impedances suffices to justify the use of mean value curves in the Nyquist diagram. The Nyquist curves of the investigated MUT depend systematically on the molding material composition. With increasing quartz sand content of the mixture, the curves approach the data of the pure quartz sand. This systematic behavior was especially observed for the mixtures of MUT 2 and for the three-component mixture of MUT 4.

Only the impedances observed for MUT 3 were not arranged in this systematic way, possibly due to poor mixing of MUT 3c. The repeated emptying and filling of the measuring cell may also have resulted in a segregation or thin-

ning of the bentonite due to an unavoidable dust removal at MUT 3c. This could have led to a drop in the bentonite concentration in the measurements carried out later in the measurement campaign. Why this effect did not also occur with MUT 2 or MUT 4 remains to be investigated.

The “median”, “mean”, and “standard deviation” features extracted from each frequency sweep and used as regeneration state indicators varied systematically with the material composition for the two-component mixtures MUT 2 and 3. In the case of the three-component mixture MUT 4, the situation was more complicated. However, even in this case, a trend could be observed. For all compounds, the features approached the values associated with the target materials MUT 1a or 1b with increasing quartz sand content, which corresponds to a higher regeneration progress. This means that the features are basically suitable to describe the regeneration progress. These findings were confirmed by the field investigations. As the regeneration progressed, the features shifted to the values of pure quartz sand. The results support the statement that the change in feature values during used-sand regeneration reflects the process progress. The graphical comparison of the three investigated features in Fig. 13 reveals this correlation for the case of batch 2.

By comparing the impedance features for the regeneration processes of batch 1 and 2, one finds that batch 1 was regenerated less than batch 2, owing to the lower whetstone speed. Also, based on the feature values, the final product of batch 1, MTP 5, was regenerated about as much as MTP 2 of batch 2. This assumption that batch 1 ended up being regenerated to the same extent as batch 2 at MTP 2 is confirmed based on the sand laboratory measurement data collected according to traditional methods described in standards of the German foundry industry. Table 7 lists the used-sand start values of these data as well as the end value of batch 1 and the values of batch 2 from MTP 2 to MTP 5.

Table 6. Relative uncertainties of the features for monitoring the used-sand regeneration, at a confidence level of 95 %.

MUT	Relative uncertainty of the features					
	Median		Mean		Standard deviation	
	Real part (%)	Imaginary part (%)	Real part (%)	Imaginary part (%)	Real part (%)	Imaginary part (%)
MTP 0	4.70	6.48	2.78	4.86	4.89	6.89
MTP 1, batch 1	7.22	6.68	3.07	2.68	7.24	2.56
MTP 2, batch 1	2.84	5.35	3.37	2.98	3.88	2.50
MTP 3, batch 1	5.87	13.59	7.80	8.97	8.33	8.40
MTP 4, batch 1	1.01	5.23	6.34	5.80	8.15	4.86
MTP 5, batch 1	1.05	4.22	4.89	4.31	6.25	3.28
MTP 1, batch 2	11.93	14.55	3.76	5.98	2.90	5.98
MTP 2, batch 2	0.52	2.05	2.16	1.90	2.69	1.58
MTP 3, batch 2	1.41	0.59	0.45	2.48	0.67	3.28
MTP 4, batch 2	2.21	0.72	2.19	1.82	2.06	2.15
MTP 5, batch 2	1.88	0.35	1.85	1.10	1.73	1.35
MUT 1a (= target)	1.26	0.53	3.01	0.61	3.22	0.63

Table 7. Reference measurement data from the sand laboratory to verify the observed characteristic data of the impedance spectra.

	Used sand	Batch 1		Batch 2			
		MTP 5	MTP 2	MTP 3	MTP 4	MTP 5	
Moisture content	%	0.45	0.06	0.07	0.01	0.0	0.0
Slurry content	%	12.3	1.1	2.3	0.7	0.3	0.3
Loss on ignition	%	4.2	0.34	0.62	0.2	0.14	0.11
Elect. conductivity	μS	498.5	103.2	170.9	69.2	40.4	40.1
Active clay content	%	8.8	1.3	2.2	0.3	0.0	0.0
Degree of oolitization	%	5.2	1.3	1.7	1.1	0.8	1.0

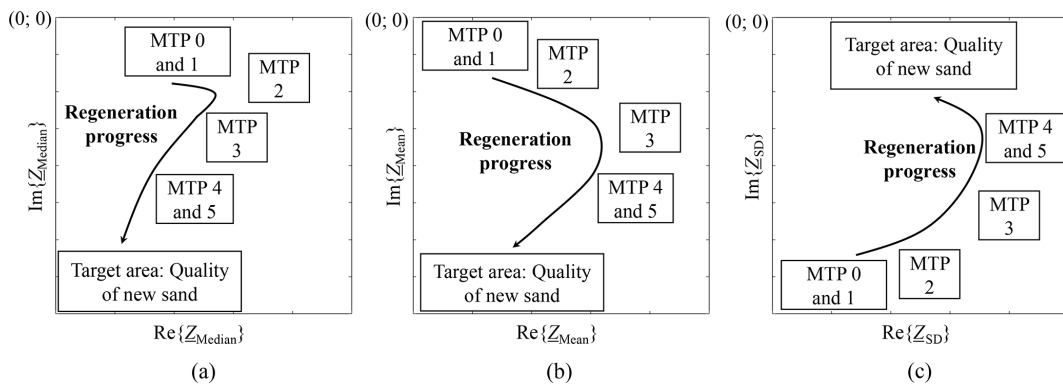


Figure 13. Impedance features as functions of the regeneration progress in batch 2. (a) “Median” feature. (b) “Mean” feature. (c) “Standard deviation” feature.

As can be seen from Figs. 10–12, the feature range of the target is not reached in this series of experiments. There are two reasons for this: first, in order to reach the target object, the quartz sand present in the used sand must be the same as that of the target object. However, since the quartz sand present in the used sand was not available in pure form, a

quartz sand with the same chemical composition but different grading curve was defined as the target object in order to be able to evaluate the tendency. On the other hand, the definition of a target object at the regeneration end depends on the foundry. A target object of “pure quartz sand” is desirable but an ideal that cannot be achieved in the real regeneration pro-

cess. Sand grains are fissured, so that carbon and bentonite particles can be deposited in the valleys on the sand grain surface, which can only be removed by completely grinding the sand grains to quartz dust. However, this is not the objective of used-sand regeneration, since quartz dust is unusable for mold production.

6 Conclusion

Based on our findings, impedance spectroscopy must be considered as a promising method for the process monitoring of used-sand regeneration in foundries. The uncertainties of the measured impedances as well as of the presented features are sufficiently low, which speaks for the reproducibility of the measurement results even when molding material conditions, i.e., new particle arrangements, vary between consecutive measurement-cell fillings.

A systematic relationship between the Nyquist curves and the composition of the MUT was sometimes difficult to recognize. The situation improved when features such as median, mean, and standard deviation of impedance spectra were used. Based on laboratory results and field measurements, these features are suitable for indicating the sand composition and thus monitoring the regeneration progress. By different regeneration of two batches, it could be shown that a slower whetstone speed leads to a lower degree of regeneration. If the whetstone speed increases, the used sand is also regenerated more strongly within the same regeneration time and better approaches the condition of pure quartz sand.

With these results, an automated online measurement system, which is directly attached to the regenerator and performs the measurements directly in the process, appears feasible. Calibration might be achieved with pure quartz sand or a target regenerate specified as such by a foundry or foundry association. The impedance features obtained with it would serve as process goal in a particular environment (foundry, regenerator, or measurement cell). It is not even necessary to extract numerical values for physical quantities (sand density and permittivity, etc.). It rather suffices to compare currently measured feature values and target values. If, unlike in this work, a direct connection between features and the investigated system is not possible, the method lends itself to the use of machine learning as already mentioned in the text.

Code and data availability. A code listing describing the programs and the data are stored in an archive and are publicly available at https://doi.org/10.15495/do_UBT_2095 (Bifano et al., 2022). If you wish to receive more information about this article, please send your request to the following e-mail address: mrt@uni-bayreuth.de.

Author contributions. LB and MW researched the background information and carried out the investigation. LB wrote the original draft. The methodology was implemented by LB, MW, AF,

GW, and GF. The project administration was conducted by AF. AF was responsible for funding acquisition. The experimental resources were procured by MW, AF, GW, and GF. Supervision, writing review, and editing were the responsibility of GF.

Competing interests. The contact author has declared that none of the authors has any competing interests.

Disclaimer. Publisher's note: Copernicus Publications remains neutral with regard to jurisdictional claims in published maps and institutional affiliations.

Special issue statement. This article is part of the special issue "Sensors and Measurement Science International SMSI 2021". It is a result of the Sensor and Measurement Science International, 3–6 May 2021.

Financial support. This research has been supported by the Bundesministerium für Wirtschaft und Energie (grant no. ZF4152305DB8).

This open-access publication was funded by the University of Bayreuth.

Review statement. This paper was edited by Beat Jeckelmann and reviewed by two anonymous referees.

References

- Al Rashid, Q. A., Abuel-Naga, H. M., Leong, E.-C., Lu, Y., and Al Abadi, H.: Experimental-artificial intelligence approach for characterizing electrical resistivity of partially saturated clay liners, *Appl. Clay Sci.*, 156, 1–10, <https://doi.org/10.1016/j.clay.2018.01.023>, 2018.
- Balmus, S.-B., Pascariu, G.-N., Creanga, F., Dumitru, I., and Sandu, D. D.: The cavity perturbation method for the measurement of the relative dielectric permittivity in the micro-wave range, *J. Optoelect. ADV M.*, 8, 971–977, 2006.
- Belyaeva, T. A., Bobrov, P. P., Kroschka, E. S., Lapina, A. S., and Rodionova, O. V.: The effect of very low water content on the complex dielectric permittivity of clays, sand-clay and sand rocks, *Meas. Sci. Technol.*, 28, <https://doi.org/10.1088/1361-6501/28/1/014005>, 2017.
- Bifano, L., Fischerauer, A., and Fischerauer, G.: Investigation of complex permittivity spectra of foundry sands, *Tech. Mess.*, 87, 372–380, <https://doi.org/10.1515/teme-2019-0121>, 2020.
- Bifano, L., Fischerauer, A., Liedtke, A., and Fischerauer, G.: Characterization of sand and sand-binder systems from foundry industry with impedance spectroscopy, *J. Sens. Sens. Syst.*, 10, 43–51, <https://doi.org/10.5194/jsss-10-43-2021>, 2021.
- Bifano, L., Weider, M., Fischerauer, A., Wolf, G., and Fischerauer, G.: MUT 1–4 and MTP 0–5/In-situ monitoring of used-sand regeneration in foundries by impedance

- spectroscopy, Universität Bayreuth [code and data set], https://doi.org/10.15495/do_ubt_2095, 2022.
- Chu, Y., Nie, S., Liu, S., Lee, C., and Bate, B.: Complex dielectric permittivity of metal and polymer modified montmorillonite, *J. Hazard Mater.*, 374, 382–391, <https://doi.org/10.1016/j.jhazmat.2019.04.066>, 2019.
- Denes, M.: Aktualisierte Umwelterklärung 2019: Daimler Truck AG Standort Mannheim (Updated Environmental Certificate 2019: Daimler Truck AG plant Mannheim; in German), Daimler, Mannheim, <https://group.mercedes-benz.com/dokumente/nachhaltigkeit/produktion/2020-06-16-uwe-mannheim-2019.pdf> (last access: 10 October 2022), 2019.
- Fieber, L., Bukhari, S. S., Wu, Y., and Grant, P. S.: In-line measurement of the dielectric permittivity of materials during additive manufacturing and 3D data reconstruction, *Addit. Manuf.*, 32, 101010, <https://doi.org/10.1016/j.addma.2019.101010>, 2020.
- Götze, J. and Göbbels, M.: Einführung in die Angewandte Mineralogie (Introduction to Applied Mineralogy; in German), Springer Spektrum, Berlin, 23–43, <https://doi.org/10.1007/978-3-662-50265-5>, 2017.
- Hilzenthaler, M., Bifano, L., Scherm, F., Fischerauer, G., Seemann, A., and Glatzel, U.: Characterization of recycled AISI 904L superaustenitic steel powder and influence on selective laser melted parts, *Powder Technol.*, 391, 57–68, <https://doi.org/10.1016/j.powtec.2021.06.011>, 2021.
- Kaden, H., Königer, F., Stromme, M., Niklasson, G. A., and Emmerich, K.: Low-frequency dielectric properties of three bentonites at different absorbed water states, *J. Colloid Interface Sci.*, 411, 16–26, <https://doi.org/10.1016/j.jcis.2013.08.025>, 2013.
- Opyd, B., and Granat, K.: The influence of sand grains properties on electrical properties of moulding sand with inorganic binder, *Arch. Foundry Engin.*, 15, 43–46, <https://doi.org/10.1515/afe-2015-0057>, 2015.
- Paradowski, L. R.: Uncertainty ellipses and their application to interval estimation of emitter position, *IEEE T. Aero. Elec. Sys.*, 33, 126–133, <https://doi.org/10.1109/7.570715>, 1997.
- Peduzzi, P.: Sand, rarer than one thinks, UN Environment Program Global Environmental Alert Service (GEAS), <https://wedocs.unep.org/handle/20.500.11822/8665> (last access: 10 October 2022), 2014.
- Robinson, D. A. and Friedman, S. P.: A method for measuring the solid particle permittivity or electrical conductivity of rocks, sediments, and granular materials, *J. Geophys. Res.*, 108, 2076, <https://doi.org/10.1029/2001JB000691>, 2003.
- Stachowicz, M.: Effect of Sand Base Grade and Density of Moulding Sands with Sodium Silicate on Effectiveness of Absorbing Microwaves, *Arch. Foundry Engin.*, 16, 103–108, <https://doi.org/10.1515/afe-2016-0059>, 2016.
- Statista: Anzahl der Eisengießereien nach ausgewählten Ländern weltweit im Jahr 2020 (Number of iron foundries by selected countries worldwide in 2020; in German), European Foundry Association, American Foundry Society, <https://de.statista.com/statistik/daten/studie/421593/umfrage/> (last access: 10 October 2022), 2020a.
- Statista: Anzahl an Gießereien nach ausgewählten Ländern weltweit im Jahresvergleich 2005 und 2020 (Number of foundries by selected countries worldwide in annual comparison 2005 and 2020; in German), European Foundry Association, American Foundry Society, <https://de.statista.com/statistik/daten/studie/421564/umfrage/anzahl-der-giessereien-nach-ausgewaehlten-laendern-weltweit/> (last access: 10 October 2022), 2020b.
- Statista: Abfallaufkommen (einschließlich gefährlicher Abfälle) (Waste production (including hazardous waste); in German), Statistisches Bundesamt, <https://www.umweltbundesamt.de/daten/ressourcen-abfall/abfallaufkommen#deutschlands-abfall> (last access: 10 October 2022), 2022a.
- Statista: Anzahl der Mülldeponien in Deutschland in den Jahren 2010 bis 2020 (Number of landfills in Germany in 2010 to 2020; in German), Statistisches Bundesamt, <https://de.statista.com/statistik/daten/studie/263063/umfrage/anzahl-der-deponien-in-deutschland/> (last access: 10 October 2022), 2022b.
- Tilch, W., Polzin, H., and Franke, M.: Praxishandbuch bentonitgebundener Formstoff (Practical manual for bentonite-bound molding material; in German), Schiele & Schön, Berlin, ISBN 978-3-7949-0947-6, 2019.
- Toth, J., Svidro, J., Dioszegi, A., and Stevenson, D.: Heat absorption capacity and binder degradation characteristics of 3d printed cores investigated by inverse Fourier thermal analysis, *Int. J. Metalcast.*, 10, 306–314, <https://doi.org/10.1007/s40962-016-0043-5>, 2016.
- Toutenburg, H. and Heumann, C.: Deskriptive Statistik (Descriptive statistics; in German), Springer, Berlin, 52–80, <https://doi.org/10.1007/978-3-540-77788-5>, 2008.
- Van de Leur, R. and Zevenhoven, C.: Characterization of the granular ceramic materials corundum and mullite by impedance spectroscopy, *J. Mater. Sci.*, 26, 4086–4091, <https://doi.org/10.1007/BF02402950>, 1991.
- Wijnker, D.: Erfahrungen beim Regenerieren von Grünsand-Kernsandgemisch im Grünsandformverfahren (Experience in regenerating green sand-core sand mixture in the green sand molding process; in German), Gießerei-Praxis, 447–458, <https://www.giesserei-praxis.de/news-artikel/artikel/erfahrungen-beim-regenerieren-von-gruensand> (last access: 10 October 2022), 2014.